

Localization of the Chaperone Domain of FKBP52*

Received for publication, March 22, 2001, and in revised form, July 19, 2001
Published, JBC Papers in Press, July 25, 2001, DOI 10.1074/jbc.M102595200

Franziska Pirkel‡, Elke Fischer‡, Susanne Modrow§, and Johannes Buchner¶¶

From the ‡Institut für Organische Chemie und Biochemie, Technische Universität München, 85747 Garching, Germany and the §Institut für Medizinische Mikrobiologie und Hygiene, Universitätsklinikum Regensburg, 93042 Regensburg, Germany

FKBP52, a multidomain peptidyl prolyl *cis/trans*-isomerase (PPIase), is found in complex with the chaperone Hsp90 and the co-chaperone p23. It displays both PPIase and chaperone activity *in vitro*. To localize these two activities to specific regions of the protein, we created and analyzed a set of fragments of FKBP52. The PPIase activity toward both peptides and proteins is confined entirely to domain 1 (amino acids 1–148). The chaperone activity, however, resides in the C-terminal part of FKBP52, mainly in the region between amino acids 264 and 400 (domain 3). Interestingly, this domain also contains the tetratricopeptide repeats, which are responsible for the binding to C-terminal amino acids of Hsp90. Competition assays with a C-terminal Hsp90 peptide suggest that the non-native protein and Hsp90 are bound by different regions within this domain.

Conversion of prolyl peptide bonds from *trans*- to *cis*-prolines often is a rate-limiting step in protein folding (1–4). In 1984, the first member of a novel class of enzymes (now called peptidyl-prolyl *cis/trans*-isomerases or short PPIases)¹ was reported to catalyze this reaction (5). To date three subfamilies of PPIases have been identified: FK506-binding proteins (FKBPs), cyclophilins, and parvulins (6–8). Both FKBPs and cyclophilins bind to and are inhibited by the immunosuppressive drugs FK506 and cyclosporin A, respectively (9, 10), and are therefore termed immunophilins.

In addition to their PPIase activity, mammalian immunophilins of higher molecular mass (>40 kDa) comprise further domains that account for additional functions. These so-called large immunophilins (FKBP52, FKBP51, and cyclophilin 40) have been found in complexes with the chaperone Hsp90 and certain client proteins such as the steroid hormone receptors in their inactive states (11–13). For steroid hormone receptor activation, several Hsp90 complexes of different compositions seem to be needed (14). The receptor interacts with Hsp70 at an early stage in this chaperone cycle. Recruitment of Hsp90 via Hop leads to the formation of an intermediate complex (Hsp90·Hop·Hsp70). The final complex of the chaperone cycle

involves Hsp90, a small acidic protein called p23, and any of the three large immunophilins FKBP51, FKBP52, and cyclophilin 40 (14). The selection of the large immunophilin present in this complex seems to depend on the substrate bound (15, 16). The basis for this differential incorporation may be due to differences in affinities of the immunophilins for Hsp90 and non-native proteins (17).

The large immunophilin that was first identified to be a component of these complexes was FKBP52 (18, 19). Sequence and hydrophobic cluster analysis suggested that FKBP52 is composed of four different domains (20). Two of these domains were suggested to be structurally related to FKBP12. The first domain (amino acids 1–148) exhibits 55% amino acid homology (21) and 49% sequence identity with FKBP12, the respective small immunophilin (20). Domain 1 of FKBP52 exhibited PPIase activity toward peptide substrates in a protease-coupled assay (22). The second domain (amino acids 149–263) exhibits 28% sequence identity with FKBP12. A marginal PPIase activity was found for this part of the protein (22). The third domain (amino acids 264–400) consists of three tetratricopeptide repeats (TPRs) (16, 23–25), and the fourth domain (amino acids 400–458) seems to contain a binding site for calmodulin (26). TPRs are degenerate sequences of 34 amino acids in length that are known to mediate protein-protein interactions (27–30). These TPRs are the elements responsible for binding to Hsp90 (24, 30–33). Apparently, all three immunophilins compete for one single binding site on the Hsp90 monomer (25). Binding is mainly mediated by electrostatic interactions between the TPR motif and the C-terminal MEEVD amino acid sequence of Hsp90. Additional amino acids N-terminal to this peptide also contribute to the binding and render specificity to the interaction between the TPR and Hsp90 (30).

Similar to Hsp90 (34) and p23 (35, 36), FKBP52 has been found to display chaperone activity. It prevents the thermal aggregation of the model substrate citrate synthase (CS) *in vitro* (17, 35). Addition of the specific inhibitor rapamycin showed that this activity is independent of its PPIase activity (35).

In the present study, we set out to localize the domain responsible for the chaperone activity of FKBP52. To this end, we analyzed a set of truncation fragments of FKBP52 concerning structure, PPIase, and chaperone activity.

Our findings show that domain 1 is exclusively responsible for its PPIase activity toward both peptide and protein substrates. The interaction with non-native protein is localized to the TPR domain. Competition experiments with a C-terminal Hsp90 peptide proved that binding of Hsp90 and substrate are not mutually exclusive.

EXPERIMENTAL PROCEDURES

Materials

Chemicals—All chemicals were obtained from Merck or ICN (Mecklenheim, Germany). The tetrapeptide for the protease-coupled and

* This work was supported by grants from the Deutsche Forschungsgemeinschaft, the Bundesministerium für Bildung, Wissenschaft, Forschung und Technologie, and the Fonds der Chemischen Industrie. The costs of publication of this article were defrayed in part by the payment of page charges. This article must therefore be hereby marked "advertisement" in accordance with 18 U.S.C. Section 1734 solely to indicate this fact.

¶¶ To whom correspondence should be addressed. Tel.: 49-89-289-13341; Fax: 49-89-289-13345; E-mail: johannes.buchner@ch.tum.de.

¹ The abbreviations used are: PPIase, peptidyl-prolyl *cis/trans* isomerase; CS, citrate synthase; FKBP, FK506-binding protein; GA, glutaraldehyde; GdmHCl, guanidinium hydrochloride; RCM-T1, reduced and *S*-carboxymethylated S54G/P55N variant of RNase T₁; TPR, tetratricopeptide repeat.

protease-free PPIase assay was from Bachem AG (Bubendorf, Switzerland).

Proteins—FKBP52 and its fragments were purified as described below. Mitochondrial pig heart CS was from Roche Molecular Biochemicals. It was stored in TE buffer (50 mM Tris, 2 mM EDTA, pH 8.0). Bovine rhodanese was from Sigma. The plasmid carrying the γ S54G/P55N variant of RNase T₁ (RCM-T1) was a kind gift of F. X. Schmid (University of Bayreuth, Bayreuth, Germany). RNase-T₁ was purified and modified as described previously (37). hFKBP12 was a kind gift of Gunther Fischer (Max Planck Institute, Halle, Germany).

Fragment Design and Expression—The fragments of rabbit FKBP52 were designed according to the domain structure determined by sequence alignment and hydrophobic cluster analysis (20). The domain boundaries were determined by protease digests and hydrophobicity plot analysis according to Kyte and Doolittle (38).

For fragment expression, the cDNAs were subcloned into the T5 expression plasmid pQE30 (Qiagen, Hilden, Germany), which allows high level expression of proteins with an N-terminal His₆ tag. The plasmids were transformed into the *Escherichia coli* strain HB101. LB medium containing 100 μ g/ml of ampicillin and 40 μ g/ml of kanamycin was inoculated with the respective stationary overnight culture. These cultures were grown at 37 °C to an A₆₀₀ of 0.4. Protein expression was induced by the addition of 1 mM isopropyl- β -D-thiogalactopyranoside. The cultures were subsequently shifted to 26 °C for 4 h. Then the cells were harvested by centrifugation at 4000 \times g for 15 min at 4 °C and lysed by incubation with 1 mg/ml of lysozyme for 30 min on ice and subsequent sonication.

Protein Purification—The histidine-tagged protein fragments were purified via a succession of nickel-nitrilotriacetic acid-agarose (equilibrated in 50 mM NaH₂PO₄, 400 mM NaCl, 20 mM imidazole, pH 8.0, elution by a step gradient to 250 mM imidazole), Resource Q (50 mM Tris, 4 mM EDTA, pH 8.0), where the protein was in the flow-through, and an Amersham Pharmacia Biotech Superdex 75-pg gel filtration column (run in 50 mM Tris, 200 mM NaCl, 4 mM EDTA, pH 8.0). The purity of all fragments was analyzed on silver stained SDS-polyacrylamide gels. No contaminating bands were detected.

The pure fragments were stored in 50 mM Tris, 2 mM EDTA, pH 7.5, at -80 °C. The concentrations were determined using the extinction coefficients for a 1 mg/ml solution in a 1-cm cuvette at 280 nm, calculated according to Gill and von Hippel (39).

Purified proteins were analyzed via size exclusion high pressure liquid chromatography and fluorescence detection. The runs were carried out using a Superdex 75 HR column with a flow rate of 0.5 ml/min in 50 mM Tris-HCl, pH 7.5, 2 mM EDTA, 200 mM NaCl. 100 μ l of a 1 μ M solution of the respective fragment were applied onto the column. The elution profile was monitored by fluorescence with an excitation wavelength of 280 nm and an emission wavelength of 330 nm.

Peptide Synthesis and Purification—The Hsp90C17 peptide (IP-PLGDEDASRMEEVD) was synthesized using a 9050 PepSynthesizer (Milligen) and Fmoc (*N*-(9-fluorenyl)methyloxycarbonyl)-protected amino acids (40) as described previously (41). The peptide was lyophilized and purified by reversed phase high performance liquid chromatography using a C2/C18 copolymer column (PepS; Amersham Pharmacia Biotech) and a gradient of 0–70% acetonitrile in 0.1% trifluoroacetic acid. Finally the peptide-containing fractions were lyophilized.

Circular Dichroism Measurements—Far UV CD measurements were performed in a J-715 spectropolarimeter with a PTC343 peltier unit (Jasco, Tokyo, Japan). After dialyzing the proteins overnight against 40 mM potassium phosphate, pH 7.5, spectra were recorded from 250 to 197 nm at a constant temperature of 20 °C in 0.1-cm quartz cuvettes. All spectra were base line corrected, and the ellipticities were calculated for a mean residue weight of 112.

The α -helix content of the respective immunophilin spectra was determined using the CD spectra deconvolution software CDNN 2.1 (bioinformatik.biochemtech.uni-halle.de/cdnn/).

To determine the thermal stability of the fragments, the CD signal was monitored at 222 nm for FKBP52, FKBP52-123, and FKBP52-234 and at 215 nm for FKBP52-1 and FKBP52-12 from 20 to 80 °C at a protein concentration of 0.25 mg/ml and a heating rate of 1 °C/min.

GdmHCl Unfolding and Refolding Transitions—To determine the stability of the FKBP52 fragments against denaturation, GdmHCl unfolding transitions were monitored by fluorescence and CD spectroscopy.

For CD measurements, the signal was monitored at 222 nm in the presence of increasing concentrations of GdmHCl. 0.35 mg/ml of the respective proteins was preincubated for 24 h at 20 °C in 10 mM sodium phosphate, pH 7.5, containing GdmHCl concentrations from 0 to 6 M.

For fluorescence measurements 5 μ g/ml of the respective fragments were incubated for 24 h at 20 °C in 50 mM Tris, pH 7.5, containing

different GdmHCl concentration. Fluorescence spectra were measured at an excitation wavelength of 280 nm from 295 to 400 nm in a Spex Fluoromax-2 fluorescence spectrometer. The respective fluorescence signals at the maximum of the difference spectrum between denatured and native protein was plotted against the respective GdmHCl concentration. The equilibrium refolding transitions were performed by incubating the fragments in 50 mM Tris, pH 7.5, 4 M GdmHCl for 6 h at 20 °C and then diluting them into different GdmHCl concentrations. The conformational state of the fragments was analyzed as described for the unfolding transitions.

PPIase Activity

Protease-coupled Peptide Assay—PPIase activity toward peptide substrates was measured by a coupled assay (5) using the synthetic peptide succinyl-Ala-Xaa-Pro-Phe-*p*-nitroanilide with Xaa being a Leu. *p*-Nitroanilide can only be cleaved off by chymotrypsin when the Xaa-Pro bond is in the *trans* configuration. The release of *p*-nitroanilide results in an increase in absorbance at 390 nm. Because FKBP52-234 was highly aggregation-prone in other buffers, these measurements were carried out in 50 mM Tris, pH 7.5, for all fragments. A Jasco V-550 UV-visible spectrophotometer with a thermostated cell holder was used at a constant temperature of 10 °C. To obtain the rate constants, the reaction kinetics were fitted using the program Sigma Plot 4.0 (SPSS Inc., Chicago, IL).

Protease-free Peptide Assay—Because some PPIases have been found to be proteolytically inactivated in the protease-coupled assay, a protease-free assay had been devised (42). The basis for this assay are the different UV-visible absorption spectra of the *cis*- and *trans*-isomers of the assay peptides when transferred from 0.47 M LiCl/trifluoroethanol into aqueous buffer solution. This change can be monitored at 330 nm. The protein concentrations and buffer conditions were identical to that of the protease-coupled assay.

RCM-T1 Refolding Assay—To measure the PPIase activity toward protein substrates, refolding experiments were performed with RCM-T1. This variant is unfolded in 100 mM Tris, pH 8.0, but refolds spontaneously upon dilution into the same buffer containing 2 M NaCl (37). The kinetics of refolding of RCM-T1 are determined by the *cis/trans*-isomerization of the Tyr³⁸-Pro³⁹ bond (37). Addition of PPIases leads to an acceleration of the reaction. The assay was performed as described previously (17, 43, 44) at 15 °C in a Spex FluoroMax-2 fluorescence spectrometer (Spex Industries, Edison, NJ) with the wavelengths being set to 268 and 320 nm for excitation and emission, respectively. The spectral bandwidths were set to 1.5 nm for excitation and 3.5 nm for emission. Under these conditions, the refolding of RCM-T1 was mono-exponential. The rate constants of the reactions were determined using the program Sigma Plot 4.0 (SPSS Inc.).

Chaperone Assays

Citrate Synthase Assay—Thermal denaturation of CS (3 μ M) was achieved by incubation at 40 °C in 40 mM Hepes, pH 7.5, for 1 h. Aggregation of CS was measured by monitoring the increase in turbidity at 360 nm in a JascoV-550 UV-visible spectrophotometer equipped with a thermostated cell holder using microcuvettes (120 μ l) with a path length of 1 cm.

Alternatively, aggregation of CS (0.15 μ M) was measured by light scattering in a Spex FluoroMax-1 fluorescence spectrometer equipped with a thermostated cell holder at 43 °C (Instruments S.A.) at an excitation and emission wavelength of 360 nm (45). For the competition assays, FKBP52 and Hsp90C17 were preincubated together for 2 min in assay buffer at 43 °C before the assay was started by the addition of CS.

Rhodanese Assay—Thermal denaturation of Rhodanese (0.3 μ M) was achieved by incubation in 40 mM sodium phosphate buffer, pH 7.4, at a temperature of 44 °C for 20–30 min. Aggregation was monitored by measuring the light scattering at 360 nm in a Spex Fluoromax-1 fluorescence spectrometer with a thermostated cell holder.

Cross-linking Assays—Chemical cross-linking of FKBP52 or FKBP52 fragments with CS was performed using glutaraldehyde (GA) as the cross-linking reagent. The optimal GA concentration was determined to be 10 mM. 4 μ g of FKBP52 or FKBP52 fragments and CS were incubated in 20 μ l of 40 mM Hepes, pH 7.5, for 5 min at 40 °C. For cross-linking, 1.6 μ l of 0.125 mM GA (in 40 mM Hepes, pH 7.5) was added, and the samples were incubated for 2 min at 37 °C.

For the kinetic experiments, 4 μ g of FKBP52 or FKBP52-123 were incubated with CS in 20 μ l of 40 mM Hepes, pH 7.5, for 5, 10, 15, or 30 min at 40 °C. After different incubation times, GA was added to an end concentration of 10 mM, and samples were incubated for 2 min at 37 °C.

To stop the cross-linking, 5 μ l of 1 M Tris-HCl, pH 8.0, was added, and

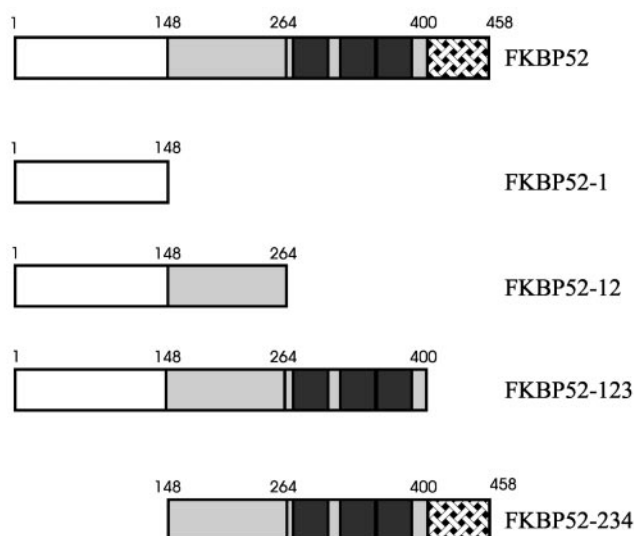


FIG. 1. **Schematic representation of FKBP52 and its fragments.** The PPIase domain is depicted in *white*, the respective TPR sites are *dark gray*, and the calmodulin binding domain is *hatched*. The domain boundaries are defined by amino acid numbers.

the samples were stored on ice. The complexes with CS were visualized by 4–12.5% gradient SDS-polyacrylamide gel electrophoresis and subsequent immunoblotting with antiserum against CS. The immunoblot was developed using ECL (Amersham Pharmacia Biotech).

Isothermal Titration Calorimetry

Titration experiments were performed using a VP isothermal titration calorimetry microcalorimeter system (MicroCal, Inc., Northampton, MA). Protein and peptide were either dialyzed into or dissolved in 40 mM Hepes, pH 7.5. In each experiment up to 26 aliquots of 5 μ l of peptide were injected into 1.43 ml of the FKBP52 solution at 25 $^{\circ}$ C. The fragment concentration in the sample cell was 20 μ M, and the concentration of injected peptide was 1.052 mM. To obtain values for ΔH , ΔS , the stoichiometry of binding and the binding constant, the titration data were fitted according to a model of one binding site using Origin software (MicroCal, Inc.) (46).

RESULTS

Fragment Design—The design of the fragments used in this study relied partially on a hydrophobic cluster analysis of the FKBP52 sequence (20), suggesting that the protein consists of four domains interspaced by short hydrophilic linkers. Proteolysis experiments and hydropathy plot analysis (38) corroborated the suggested domain boundaries (data not shown). To functionally dissect FKBP52, we cloned the fragments shown in Fig. 1. Fragment FKBP52-1 represents domain 1 of FKBP52 including the PPIase activity (22). FKBP52-234 represents the fragment that lacks domain 1. FKBP52-12 consists of domains 1 and 2 but lacks the TPR domain and the calmodulin-binding site. FKBP52-123 only lacks the C-terminal calmodulin-binding domain. All these fragments were expressed in *E. coli* and purified to homogeneity. Only FKBP52-234 tended to aggregate at concentrations higher than 0.5 mg/ml. Purification of fragments consisting of domain 2 or domain 3 alone was not possible. This is consistent with low yield obtained before for the respective glutathione *S*-transferase fusions (22).

Purified fragments were analyzed via size exclusion. All fragments were found to be monomer with the exception of FKBP52-1, which behaved like a dimer (data not shown). This is consistent with earlier findings by Yem and colleagues (47). The single domain immunophilin FKBP12 analyzed under the same conditions also behaved as a dimer.

Structure and Stability of FKBP52 Fragments—To obtain insights into the structural properties of the respective fragments of FKBP52, far UV CD measurements were performed.

TABLE I
Structure and stability of FKBP52 fragments

Far UV CD spectra and temperature transitions were performed as described under “Experimental Procedures.” The secondary structure contents were calculated using the CD spectra deconvolution software CDNN 2.1.

Fragment	α -Helix	β -Structure	Nonperiodic structure	T_m
	%	%	%	$^{\circ}$ C
FKBP52	30	36	34	49 \pm 0.6
FKBP52-1	12	58	30	68 \pm 1
FKBP52-12	13	57	31	63 \pm 0.8
FKBP-123	26	39	35	46 \pm 0.8
FKBP52-234	36	32	32	39 \pm 0.5

The spectra for FKBP52, FKBP52-123, and FKBP52-234 display two clear minima at 208 and 222 nm with intensities of -8000 to -14000 deg cm^2 dmol^{-1} . FKBP52-1 and FKBP52-12 had very little helical structure, and FKBP52-1 displayed an additional maximum at about 220 nm, which may be due to aromatic amino acids, *e.g.* phenylalanines (48). The respective secondary structure contents of these fragments are shown in Table I. Full-length FKBP52 and FKBP52-123 have an α -helix content of 30 and 26%, respectively, whereas FKBP52-234 has 36% helical structure. FKBP52-1 and FKBP52-12 display an α -helical content of only 12 and 13%, respectively. Thus, domains 3 and 4 seem to consist mainly of α -helices, whereas domains 1 and 2 are made up of β -sheets.

To investigate the stability of the fragments, temperature transitions were monitored by far UV CD as described under “Experimental Procedures.” The midpoints of denaturation (T_m) obtained from these measurements are shown in Table I. The least stable fragment was FKBP52-234 with a denaturation midpoint of 39 $^{\circ}$ C; the T_m of FKBP52-1 was 68 $^{\circ}$ C, and that of FKBP52-12 was 63 $^{\circ}$ C. The full-length FKBP52 showed a midpoint of 49 $^{\circ}$ C. When domain 4 was removed, the remaining fragment FKBP52-123 still had a midpoint of denaturation of 46 $^{\circ}$ C. This suggests that mainly domain 3 is responsible for the instability of FKBP52 against thermal denaturation and that domain 1 is the domain that provides most of the stability.

Additionally, the stability of the FKBP52 fragments was monitored by equilibrium GdmHCl transitions by CD and fluorescence spectroscopy (Fig. 2 and data not shown). The respective midpoints of denaturation were 1.8 M GdmHCl (FKBP52-1), 1.7 M GdmHCl (FKBP52-12), 1.6 M GdmHCl (FKBP52-123), 1.5 M GdmHCl (FKBP52), and 1.2 M GdmHCl (FKBP52-234). All transitions were reversible (data not shown). Taken together, these measurements suggested that both FKBP52-1 and FKBP52-12 are more stable than the other fragments and the full-length protein and thereby confirmed the results obtained from the thermal denaturation measurements.

PPIase Activity of Full-length FKBP52 and Its Fragments—The PPIase activity of various fragments of FKBP52 had been analyzed previously (22) using glutathione *S*-transferase-fused FKBP52 fragments and the protease-coupled peptide assay (5). These experiments suggested that FKBP52-1 is mainly responsible for the PPIase activity of FKBP52. However, the authors also reported marginal PPIase activity (k_{cat}/K_m is 0.02×10^6 $\text{M}^{-1} \text{s}^{-1}$) for FKBP52-2 (22).

Recently, it was shown that the protease chymotrypsin, which is used as a helper protease in this assay, can lead to the inactivation and degradation of certain PPIases in the protease-coupled assay (49). To be able to rule out effects of the protease on the different FKBP52 fragments in our study, we employed a new, protease-free assay system (42). All fragments containing domain 1 showed k_{cat}/K_m values ranging from 1.25 to 1.6×10^6 $\text{M}^{-1} \text{s}^{-1}$ for the tetrapeptide succinyl-Ala-Leu-Pro-Phe-paranitroanilide in both the protease-coupled and the pro-

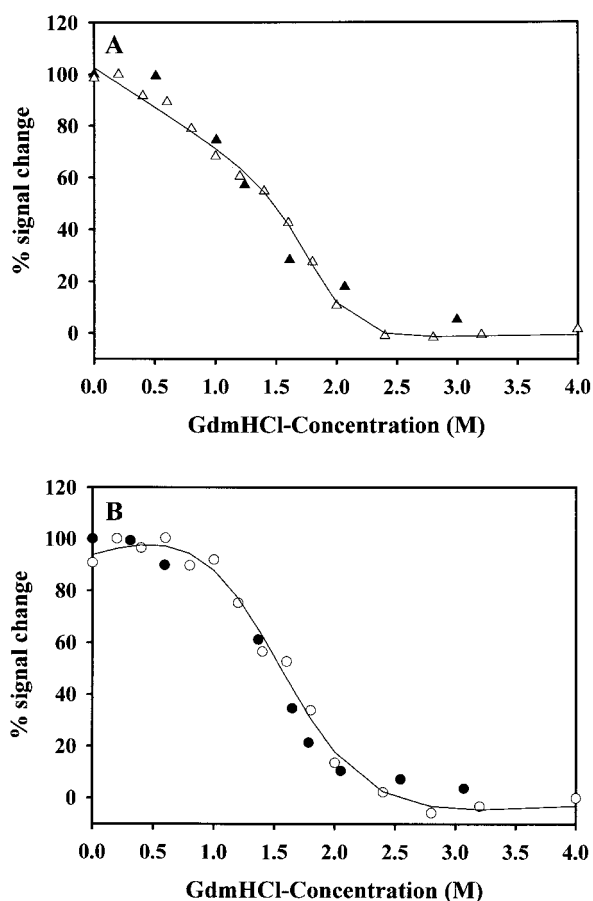


FIG. 2. **GdmHCl-induced unfolding transitions of FKBP52 fragments.** Unfolding transitions of FKBP52 and FKBP52-123 were monitored by the intrinsic fluorescence emission and CD measurements. The lines represent respective fits of the transitions. The respective midpoints of denaturation were 1.6 M GdmHCl (FKBP52-123) and 1.5 M GdmHCl (FKBP52). The fits were performed according to Santoro and Bolen (58). A, unfolding transition of FKBP52 followed by intrinsic fluorescence emission (Δ) and CD measurement (\blacktriangle). B, unfolding transition of FKBP52-123 (\circ) intrinsic fluorescence emission and CD measurement (\bullet).

tease-free assay (Fig. 3 and Table II). Thus, it is unlikely that the protease used in the protease-coupled assay inactivates regions of FKBP52 responsible for PPIase activity. The catalytic activity we found for FKBP52 and the fragments containing domain 1 in our study corresponds very well to the activities found for large human FKBP5s ($1.45 \times 10^6 \text{ M}^{-1} \text{ s}^{-1}$) that we had reported earlier (17) and to the activity of the corresponding small immunophilin FKBP12 ($2.2 \times 10^6 \text{ M}^{-1} \text{ s}^{-1}$; Ref. 50). FKBP52-234 showed no PPIase activity in either assay. Thus, our results corroborate the identification of FKBP52-1 as the domain responsible for the PPIase activity. However, we could not detect PPIase activity for domain 2.

In a second approach, we tested the PPIase activity of FKBP52 fragments in the refolding of a protein. The substrate we used for these measurements was RCM-T1 (37, 43, 44). This substrate is unfolded in 100 mM Tris, pH 8.0, and refolds spontaneously upon dilution into the same buffer containing 2 M NaCl. The rate-limiting step in this refolding reaction is the isomerization of the Tyr³⁸–Pro³⁹ peptide bond, which is in the *cis*-conformation in the native state. The reaction follows a single exponential kinetic. Addition of PPIases accelerates the rate of the refolding reaction (Fig. 4). In this assay, k_{cat}/K_m values of $5.23\text{--}5.39 \times 10^3 \text{ M}^{-1} \text{ s}^{-1}$ were determined for the full-length FKBP52 and its fragments FKBP52-1, FKBP52-12, and FKBP52-123 (Table II). These values are lower than those

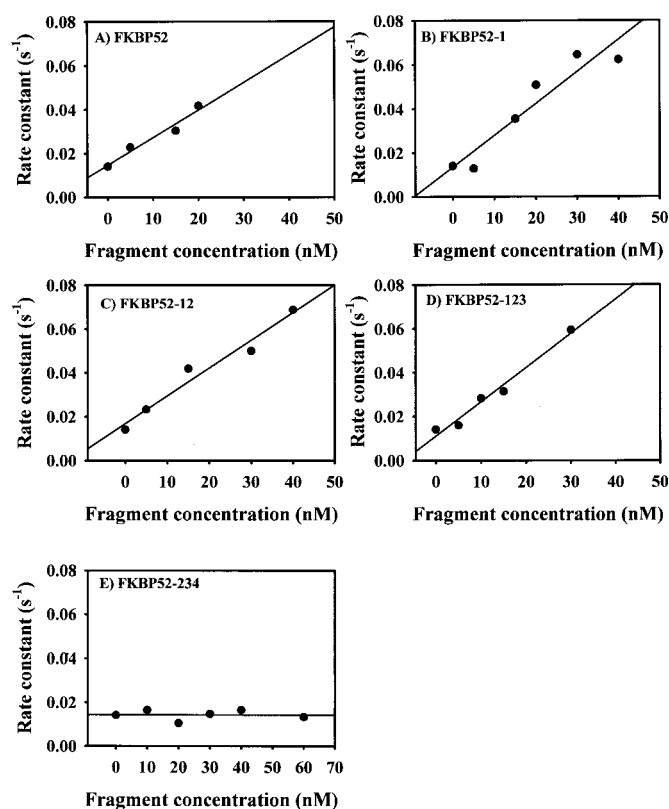


FIG. 3. **PPIase activity of FKBP52 fragments in the protease-free peptide assay.** Rate constants of the isomerization of the synthetic peptide succinyl-Ala-Leu-Pro-Phe-paranitroanilide as a function of the fragment concentration. Experiments were carried out in 50 mM Tris, pH 7.5, at 10 °C. Isomerization was monitored by the decrease in absorbance at 330 nm. The rate constants of the respective isomerization kinetics were plotted against the fragment concentration. The slope of the linear regression is equivalent to k_{cat}/K_m as summarized in Table II. A, FKBP52; B, FKBP52-1; C, FKBP52-12; D, FKBP52-123; E, FKBP52-234.

determined for human FKBP51 and FKBP52 (8.02 and $8.9 \times 10^3 \text{ M}^{-1} \text{ s}^{-1}$, respectively; Ref. 17) and only about half of the catalytic activity of the respective small immunophilin FKBP12 ($1.3 \times 10^4 \text{ M}^{-1} \text{ s}^{-1}$, 43). Again, FKBP52-234 did not have any activity in this assay (Table II). Taken together, these results show that amino acids 1–148 (domain 1) are both necessary and sufficient for wild type-like PPIase activity toward both peptide and protein substrates.

Chaperone Activity of FKBP52 and Its Fragments—To monitor the chaperone activity of the FKBP52 fragments, the CS aggregation assay was used (45). At temperatures above 37 °C, CS starts to aggregate spontaneously. FKBP52-234 could not be used in this assay, because it started to aggregate irreversibly at about this temperature (Table I).

As shown previously, an excess of FKBP52 inhibited the aggregation of CS effectively (Refs. 17 and 35 and Fig. 5A). Similar results were obtained for FKBP52-123 (Fig. 5B). However, fragment FKBP52-123 does not seem to be quite as potent a chaperone as the full-length protein because CS aggregation could not be suppressed completely by this fragment. Interestingly, addition of FKBP52-12 did not influence the aggregation behavior of CS, even when added in high excess over CS (Fig. 5C). This suggests that domain 3, which consists predominantly of TPRs, is mainly responsible for the chaperone activity of FKBP52, even though the C-terminal 58 amino acids seem to have a slight additional effect.

Complex formation between non-native CS and FKBP52 fragments was directly examined by cross-linking with GA.

TABLE II
PPIase activities of FKBP52 fragments

The PPIase activities were measured as described under "Experimental Procedures." The k_{cat}/K_m values were determined from the slopes of the respective linear regression as shown in Figs. 2 and 3 for all of the fragments examined. Dashes indicate no PPIase activity.

FKBP52 fragment	k_{cat}/K_m in the protease-coupled peptide assay	k_{cat}/K_m in the protease-free peptide assay	k_{cat}/K_m in the RCM-T1-refolding assay
	$M^{-1} s^{-1}$	$M^{-1} s^{-1}$	$M^{-1} s^{-1}$
FKBP52 (full length)	$1.45 \pm 0.21 \times 10^6$	$1.25 \pm 0.21 \times 10^6$	$5.23 \pm 0.1 \times 10^3$
FKBP52-123	$1.60 \pm 0.24 \times 10^6$	$1.42 \pm 0.20 \times 10^6$	$5.28 \pm 0.1 \times 10^3$
FKBP52-12	$1.33 \pm 0.30 \times 10^6$	$1.25 \pm 0.26 \times 10^6$	$5.39 \pm 0.09 \times 10^3$
FKBP52-1	$1.50 \pm 0.22 \times 10^6$	$1.55 \pm 0.31 \times 10^6$	$5.35 \pm 0.08 \times 10^3$
FKBP52-234	—	—	—

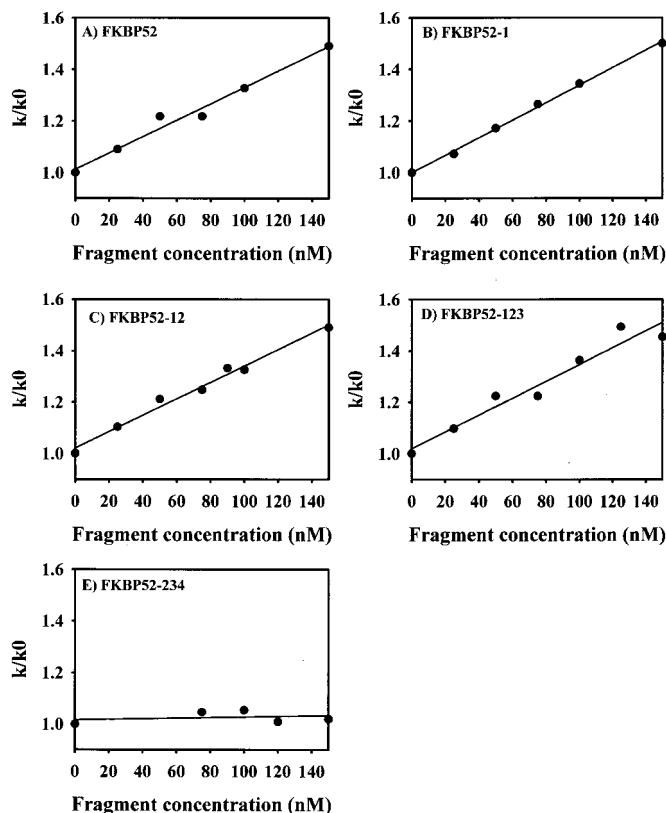


FIG. 4. PPIase activity of the FKBP52 fragments in the refolding of RCM-T1. Ratios of the observed rate constants for the refolding of RCM-T1 in the presence (k) and the absence (k_0) of PPIase depicted as a function of the respective fragment concentration. The k_{cat}/K_m values were calculated by multiplying the slope of the respective linear regression with k_0 . A, FKBP52; B, FKBP52-1; C, FKBP52-12; D, FKBP52-123; E, FKBP52-234.

Previously this methodology had been employed to demonstrate complex formation between CS and the full-length FKBP52 (35). Here, we could confirm this interaction. In addition, specific complexes were observed by cross-linking between CS and fragment FKBP52-123, which contains the postulated chaperone domain. In contrast, fragment FKBP52-12, which lacks this domain, did not show complex formation with CS (Fig. 6A). The complexes seem to be stable because prolonged incubation at 40 °C (Fig. 6, B and C) or 25 °C (data not shown) did not lead to changes in the amount of CS bound.

To test whether the chaperone activity of FKBP52 is broad, we also monitored its influence on rhodanese, another well established chaperone substrate (51). Upon incubation at 44 °C, rhodanese aggregates readily over a period of 20 min (Fig. 7). Addition of FKBP52 in a 5-fold excess led to about half-maximal suppression of aggregation (Fig. 7A). Increasing the FKBP52 concentration further reduced aggregation. However, complete suppression of aggregation was not achieved

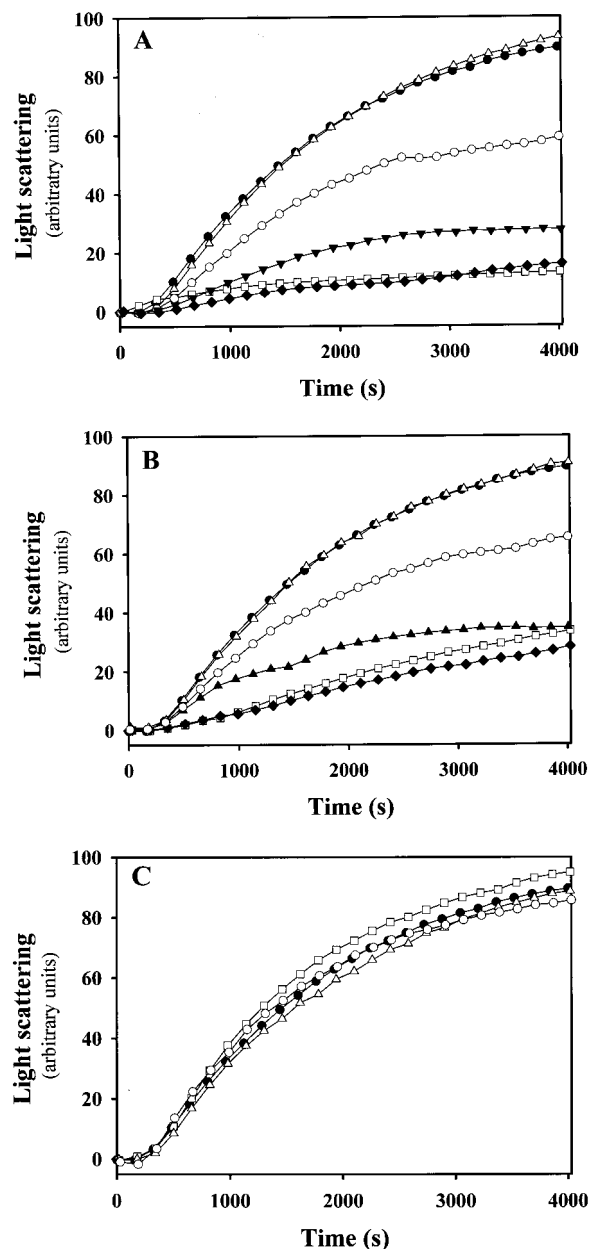


FIG. 5. Influence of FKBP52 fragments on the thermal aggregation of CS. CS was incubated at 40 °C. Aggregation was monitored by measuring the turbidity of the solution at 360 nm in the absence and the presence of additional components as described under "Experimental Procedures." A, aggregation of CS in the absence of additional components (●) and in the presence of 3 μM (Δ), 6 μM (○), 12 μM (▼), 24 μM (◆), and 33 μM (□) full-length FKBP52. B, aggregation of CS in the absence of additional components (●) and in the presence of 3 μM (Δ), 6 μM (○), 9 μM (▲), 24 μM (◆), and 30 μM (□) FKBP52-123. C, aggregation of CS in the absence of additional components (●) and in the presence of 15 μM (○), 30 μM (□), and 42 μM (Δ) of FKBP52-12.

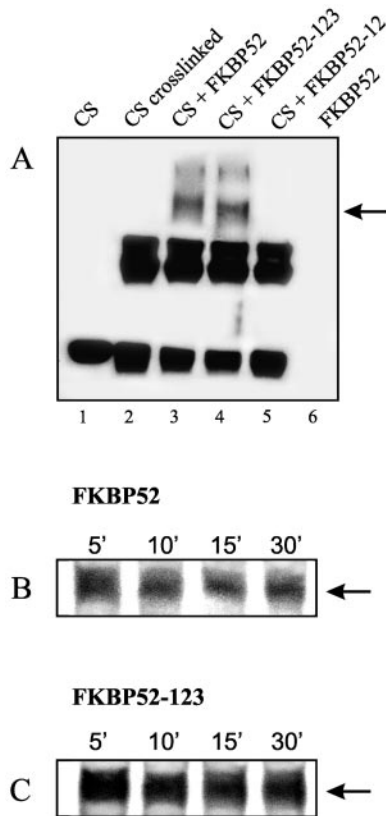


FIG. 6. Cross-linking of CS with FKBP52 and FKBP52 fragments. Complexes between FKBP52 or FKBP52 fragments and CS are shown. *A*, complex formation between FKBP52, FKBP52-123, or FKBP-12 and CS after incubation for 5 min at 40 °C was demonstrated by cross-linking with GA and subsequent immunoblotting with antibody against CS. *Lane 1* contains CS not cross-linked with GA; *lanes 2–5* contain cross-linked samples of the proteins indicated above; and *lane 6* contains cross-linked FKBP52, which is not recognized by the antibody against CS. *B*, stability of the complex between FKBP52 and CS. GA was added after 5, 10, 15, and 30 min of incubation at 40 °C. *C*, stability of the complex between FKBP52-123 and CS. GA was added after 5, 10, 15, and 30 min of incubation at 40 °C.

even at high excess. As already shown for CS, FKBP52-123 also suppressed the aggregation of rhodanese (Fig. 7*B*). Addition of FKBP51-12 did not have any effect on rhodanese aggregation even when added in high excess (Fig. 7*C*). IgG, added as a control, did not influence rhodanese aggregation (Fig. 7*B*). Thus, the rhodanese assays confirm the results obtained from the CS measurements.

Binding of the Peptide Hsp90C17 to FKBP52—Earlier studies (16, 23, 24, 25) had shown that the TPRs of FKBP52 are localized in domain 3. These TPRs have been proven to be involved in the binding of the large immunophilins to Hsp90 (24, 31). To determine directly whether the C-terminal region of Hsp90 binds to FKBP52, we synthesized a peptide (Hsp90C17) comprising 17 C-terminal residues of Hsp90 (IP-PLGDEASRMEEVD). This includes the MEEVD motif, which is absolutely necessary for the binding of Hsp90 to the TPR domain of Hop (30) and 12 additional amino acids to enforce the binding and render specificity to it.

Binding of the Hsp90 peptide Hsp90C17 to FKBP52 was monitored by isothermal titration calorimetry (Fig. 8). The binding curves obtained were sigmoidal, which is consistent with a simple two-state association reaction. The binding constant of Hsp90C17 to FKBP52 was determined to be 3 μM (Fig. 8). This is consistent with the binding constants determined for the binding of Hsp90 peptides to the TPR domain of Hop before (30). The binding of FKBP52 to the Hsp90C17 peptide had both

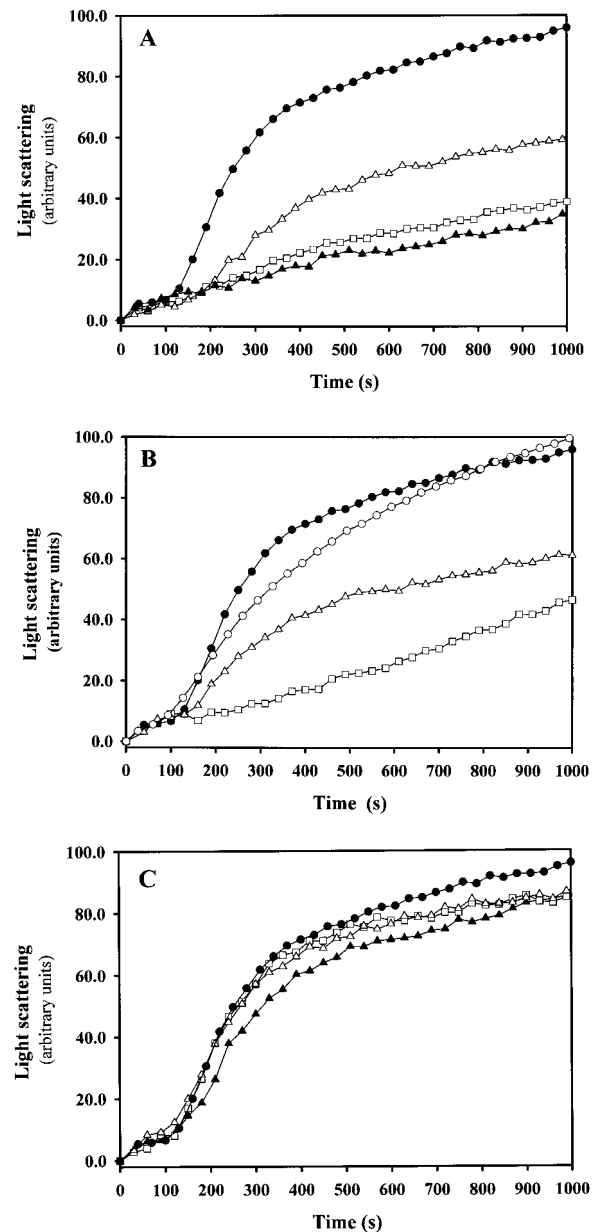


FIG. 7. Influence of FKBP52 fragments on the thermal aggregation of rhodanese. Rhodanese (0.3 μM) was incubated for 30 min at 44 °C. Aggregation was monitored by measuring the light scattering in the solution at 360 nm in the absence and the presence of additional components as described under “Experimental Procedures.” *A*, aggregation of rhodanese in the absence of additional components (●) and in the presence of 1.5 μM (△), 3 μM (□), or 6 μM (▲) of FKBP52. *B*, aggregation of rhodanese in the absence of additional components (●) and in the presence of 1.5 μM (△) and 3 μM (□) of FKBP52-123. IgG (30 $\mu\text{g}/\text{ml}$) used as a control (○) did not have any influence on the aggregation of rhodanese. *C*, aggregation of rhodanese in the absence of additional components (●) and in the presence of 1.5 μM (△), 3 μM (□), and 6 μM (▲) of FKBP52-12.

a favorable entropic ($T\Delta S = 5.5$ kcal/mol) and enthalpic (-2.1 kcal/mol) contribution. The stoichiometry of binding was 0.8. In contrast to FKBP52, the peptide did not bind to FKBP52-12 (Fig. 8), corroborating that this peptide binds specifically to the TPR domains.

Competition Measurements with FKBP52 and Hsp90C17 in the CS Assay—To determine whether binding to the non-native protein and binding to Hsp90 were mutually exclusive or whether the substrate protein and Hsp90 bound to different structures in the same region of FKBP52, we devised a competition assay to check whether Hsp90C17 inhibited the interac-

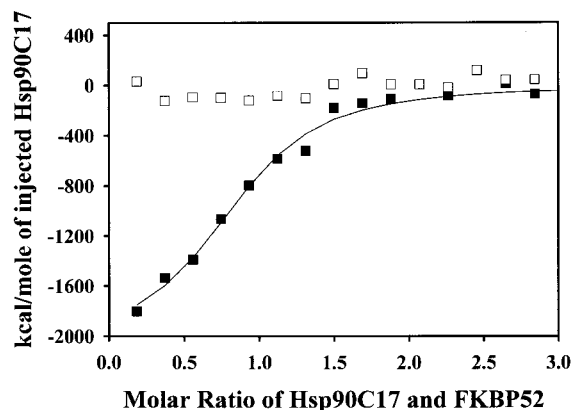


FIG. 8. **Interaction between FKBP52 and Hsp90C17, a peptide derived from the 17 C-terminal amino acids of Hsp90.** Isothermal titration calorimetry was performed in 40 mM Hepes, pH 7.5, at 25 °C. The FKBP52 concentration in the cell was 20 μ M, and the concentration of Hsp90C17 was 1.052 mM in the syringe. 5 μ l of the peptide solution were injected 26 times. The data were fitted to a model of one binding site using the Origin Software (MicroCal, Inc.). The figure shows the enthalpy per mole of Hsp90C17 injected plotted versus the molar ratio of FKBP52 (■) and FKBP52-12 (□) in the sample cell to Hsp90C17 injected.

tion of FKBP52 with CS. To this end, FKBP52 and Hsp90C17 were preincubated together at 43 °C. The assay was started by the addition of CS. Hsp90C17 was added in a 10-fold excess over FKBP52. Given the binding constants determined in the isothermal titration calorimetry experiment, FKBP52 was saturated with peptide. If there was a competition of CS and Hsp90 for a common binding site on FKBP52, a decrease in the chaperone activity of FKBP52 should now be detectable. However, Hsp90C17 did not have any effect on the chaperone activity of FKBP52 (Fig. 9). FKBP52 suppressed CS aggregation both in presence and in absence of 30 μ M of Hsp90C17. Hsp90C17 alone added as a negative control did not influence the aggregation behavior of CS.

DISCUSSION

FKBP52 is a large immunophilin that acts as a co-factor of Hsp90 and exhibits both PPIase and chaperone activity (35). In this study we set out to determine the regions of FKBP52 responsible for these activities. We designed a set of fragments of FKBP52 and compared them concerning structure, stability, PPIase, and chaperone activity. FKBP52 consists of four domains that show distinct amounts of α -helical content. Domains 3 and 4 seem to be largely made up of α -helices, whereas domains 1 and 2 only contain a limited amount of α -helical structure (~ 12%). These domains share sequence homology with FKBP12 (20), which displays also about 10% α -helical structure (17). The high α -helix content of domains 3 and 4 reflects the presence of the helical structures of the calmodulin-binding domain (52) and the TPRs (29, 30).

There was no difference in the catalytic activity in the protease-coupled and the protease-free variant of the peptide assay, which suggests that the helper protease chymotrypsin does not inactivate FKBP52. The PPIase activity of FKBP52 and the fragments containing domain 1 corresponds very well with the activities found for FKBP51 and FKBP52, which we had reported earlier (17), and with the activity of the corresponding small immunophilin FKBP12 (50). In the catalysis of refolding of the protein substrate RCM-T1, the activity of FKBP52 is about half of the catalytic activity of the respective small immunophilin FKBP12 (43). In both assays, only fragments containing domain 1 display PPIase activity, indicating that amino acids 1–148 are both necessary and sufficient for wild type-like PPIase activity toward both peptide and protein

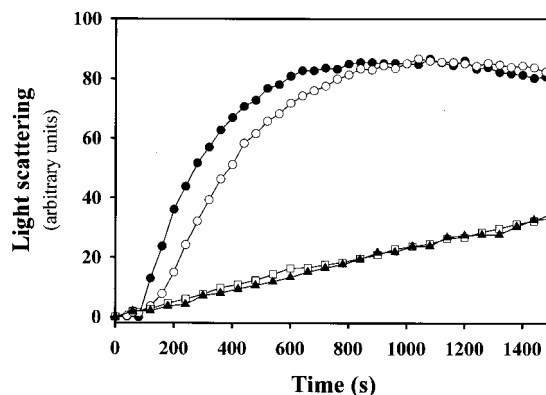


FIG. 9. **Chaperone assays in the presence of FKBP52 and peptide.** CS aggregation assays were performed at 43 °C. Aggregation was monitored at 360 nm. Measurements were carried out in absence of additional components (●) and in the presence of 3 μ M FKBP52 alone (□) and in the presence of 3 μ M FKBP52 and 30 μ M Hsp90C17 (▲). The addition of 30 μ M Hsp90C17 (○) alone as a control did not influence CS aggregation.

substrates. In contrast to the findings of Chambraud *et al.* (22), we did not detect PPIase activity for domain 2 in either assay.

The ribosome-associated trigger factor of *E. coli* is another large PPIase consisting of a FK506-binding domain and additional domains. These additional domains are involved in the interaction with substrate proteins such as RCM-T1, which causes a greatly enhanced catalytic activity in the refolding of RCM-T1 compared with the small PPIases (53). In contrast to this, the additional domains of FKBP52 do not have any influence on the catalytic efficiency of prolyl-peptide bond isomerization in RCM-T1 refolding. This suggests that in contrast to trigger factor, in FKBP52 only the PPIase domain is involved in the refolding of RCM-T1.

In addition to being a PPIase, FKBP52 has also been shown to display chaperone activity *in vitro* (17, 35). It has been suggested that the chaperone activity resides in domains outside the PPIase domain (35). Interestingly, for a thermophilic single domain FKBP, it was shown that insertions in this PPIase domain are important for chaperone-like activity (54). In contrast, using two well established model substrates, CS and rhodanese, we were able to localize the site for interaction with non-native proteins to the C-terminal part of FKBP52 in this study. It is mainly localized between amino acids 264 and 400. However, the C-terminal 58 amino acids also seem to contribute because fragment FKBP52-123 did not completely suppress CS aggregation. Because large FKBP52s are found predominantly in complex with Hsp90 *in vivo*, the ability of FKBP52 to interact with non-native proteins, as analyzed *in vitro*, may contribute to the conformational processing of substrates in the Hsp90 complex. However, the *in vivo* importance of prolyl isomerization or binding of substrate proteins by FKBP52 remains to be established in the Hsp90 complex.

In FKBP52, the TPR domain is involved in the binding to Hsp90 (24, 31). Because the binding site for proteins in FKBP52 co-localizes with the TPR domain, the question arose whether non-native protein and Hsp90 bind to the same site on FKBP52. To address this, we performed CS aggregation measurements in the presence of a C-terminal 17-residue Hsp90 peptide bound to FKBP52. The binding constant of this peptide to FKBP52 was determined to be 3 μ M. This affinity corresponds well to that of Hsp90 C-terminal peptides to the TPR2A region of Hop (30), which is homologous to the TPR region of FKBP52. However, the Hop TPR2A region bound equally well to C-terminal Hsp90 peptides longer than 10 amino acids and to the entire C-terminal domain (amino acids 625–732) of Hsp90, whereas the binding affinity of the 17-amino acid

Hsp90 peptide to FKBP52 is markedly lower than the one determined for the binding between FKBP52 and full-length Hsp90 ($K_D = 55$ nM; Ref. 17). This argues for the involvement of more than the C-terminal 17 amino acids of Hsp90 and the TPR domain of FKBP52 in the binding of FKBP52 and Hsp90 as had been suggested before (16).

The presence of the Hsp90 peptide at saturating conditions did not have any effect on the suppression of CS aggregation by FKBP52. This suggests that both proteins can bind to domain 3 of FKBP52 at the same time and that their binding is not mutually exclusive.

The structural basis of the interaction between the C-terminal peptides of Hsp90 and the TPR domain of Hop, which is homologous to FKBP52 is already known (30). Similar to the TPR structure of the phosphatase PP5 in the absence of binding peptide (29), it consists of seven meandering α -helices that form a cradle-shaped groove. This groove accommodates the peptide in an extended conformation. The peptide only makes contact with the side chains of the three α -helices of the TPR domain that line the inner surface of the groove (30). In this structure a considerable part of the groove is not occupied by the Hsp90 peptide and may thus remain accessible to other proteins. A comparison between the TPR domains of Hop and the TPRs of FKBP52 shows that both the residues belonging to the TPR consensus motif and the residues that were found to be responsible for electrostatic interactions with the C-terminal EEVD peptide of Hsp90 are highly conserved (30). Apart from this, however, the homology between the respective TPR domains of the two proteins is not very high (only 14% overall amino acid identity in the TPR2A region). Moreover, the loop between helix 1B and 2A contains 15 additional amino acids in FKBP52. In contrast to FKBP52, Hop does not bind to non-native proteins (35, 36). This provides additional support for the conclusion that it is not the Hsp90 interacting TPR, which is responsible for binding of the non-native protein.

Generally, TPR motifs are thought to mediate a specific protein-protein interaction via a defined set of interactions of eight loosely conserved residues (28, 55). A wider binding specificity of TPR regions was suggested for the mitochondrial import receptor protein Tom70 concerning presequence peptides (56). Surprisingly, the TPR was part of the binding site of Tom20 for the preprotein, but the TPR motif itself did not form the recognition element for the presequence (57). Instead, the basis for binding was a patch of hydrophobic interactions, only part of which was localized in the TPR helices. Such a hydrophobic patch could also mediate interactions with non-native proteins in FKBP52.

Acknowledgments—We thank B. Chambrud for information on the domain structure of FKBP52. Additionally, we are grateful to Klaus Richter for advice with the isothermal titration calorimetry measurements and to Astrid Brunner for peptide synthesis.

REFERENCES

- Brandts, J. F., Halvorson, H. R., and Brennan, M. (1975) *Biochemistry* **14**, 4953–4963
- Schmid, F. X., and Baldwin, R. L. (1978) *Proc. Natl. Acad. Sci. U. S. A.* **75**, 4764–4768
- Kim, P. S., and Baldwin, R. L. (1982) *Annu. Rev. Biochem.* **51**, 459–489
- Schmid, F. X. (1993) *Annu. Rev. Biophys. Biomol. Struct.* **22**, 123–143
- Fischer, G., Bang, H., and Mech, C. (1984) *Biomed. Biochim. Acta* **43**, 1101–1111
- Fischer, G. (1994) *Angew. Chem. Int. Ed. Engl.* **33**, 1415–1436
- Göthel, S. F., and Marahiel, M. A. (1999) *Cell. Mol. Life Sci.* **55**, 423–436
- Schiene, C., and Fischer, G. (2000) *Curr. Opin. Struct. Biol.* **10**, 40–45
- Handschumacher, R. E., Harding, M. W., Rice, J., Drugge, R. J., and Speicher, D. W. (1984) *Science* **226**, 544–546
- Harding, M. W., Galat, A., Uehling, D. E., and Schreiber, S. L. (1989) *Nature* **341**, 761–763
- Smith, D. F., Faber, L. E., and Toft, D. O. (1990) *J. Biol. Chem.* **265**, 3996–4003
- Pratt, W. B., and Toft, D. O. (1997) *Endocr. Rev.* **18**, 306–360
- Buchner, J. (1999) *Trends Biochem. Sci.* **24**, 136–141
- Smith, D. F. (1998) *Biol. Chem.* **379**, 283–288
- Nair, S. C., Rimerman, R. A., Toran, E. J., Chen, S., Prapapanich, V., Butts, R., and Smith, D. F. (1997) *Mol. Cell. Biol.* **17**, 594–603
- Barent, R. L., Nair, S. C., Carr, D. C., Ruan, Y., Rimerman, R. A., Fulton, J., Zhang, Y., and Smith, D. F. (1998) *Mol. Endocrinol.* **12**, 342–354
- Pirkel, F., and Buchner, J. (2001) *J. Mol. Biol.* **308**, 795–806
- Tai, P. K., Maeda, Y., Nakao, K., Wakin, N. G., Duhring, J. L., and Faber, L. E. (1986) *Biochemistry* **25**, 5269–5275
- Renoir, J.-M., Radanyi, C., Faber, L. E., and Baulieu, E.-E. (1990) *J. Biol. Chem.* **265**, 10740–10745
- Callebaut, I., Renoir, J.-M., Lebeau, M.-C., Massol, N., Burny, A., Baulieu, E.-E., and Mornon, J.-P. (1992) *Proc. Natl. Acad. Sci. U. S. A.* **89**, 6270–6274
- Lebeau, M.-C., Massol, N., Herrick, J., Faber, L., Renoir, J.-M., Radanyi, C., and Baulieu, E.-E. (1992) *J. Biol. Chem.* **267**, 4281–4284
- Chambrud, B., Rouviere-Fourmy, N., Radanyi, C., Hsiao, K., Peattie, D. A., Livingston, D. J., and Baulieu, E. E. (1993) *Biochem. Biophys. Res. Commun.* **196**, 160–166
- Owens-Grillo, J. K., Hoffmann, K., Hutchinson, K. A., Yem, A. W., Deibel, M. R., Jr., Handschumacher, R. E., and Pratt, W. B. (1995) *J. Biol. Chem.* **270**, 20479–20484
- Radanyi, C., Chambrud, B., and Baulieu, E. E. (1994) *Proc. Natl. Acad. Sci. U. S. A.* **91**, 11197–11207
- Ratajczak, T., and Carrello, A. (1996) *J. Biol. Chem.* **271**, 2961–2965
- Massol, N., Lebeau, M.-C., Renoir, J.-M., Faber, L. E., and Baulieu, E.-E. (1992) *Biochem. Biophys. Res. Commun.* **187**, 1330–1335
- Sikorski, R. S., Boguski, M. S., Goebel, M., and Hieter, P. (1990) *Cell* **60**, 307–317
- Lamb, J. R., Tugendreich, S., and Hieter, P. (1995) *Trends Biochem. Sci.* **20**, 257–259
- Das, A. K., Cohen, P. T., and Barford, D. (1998) *EMBO J.* **17**, 1192–1199
- Scheufler, C., Brinker, A., Bourenkov, G., Pegoraro, S., Moroder, L., Bartunik, H., Hartl, F. U., and Moarefi, I. (2000) *Cell* **101**, 199–210
- Hoffman, K., and Handschumacher, R. E. (1995) *Biochem. J.* **307**, 5–8
- Young, J. C., Obermann, W. M., and Hartl, F. U. (1998) *J. Biol. Chem.* **273**, 18007–18010
- Carrello, A., Ingley, E., Minchin, R. F., Tsai, S., and Ratajczak, T. (1999) *J. Biol. Chem.* **274**, 2682–2689
- Wiech, H., Buchner, J., Zimmermann, R., and Jakob, U. (1992) *Nature* **358**, 169–170
- Bose, S., Weikl, T., Bügl, H., and Buchner, J. (1996) *Science* **274**, 1715–1717
- Freeman, B. C., Toft, D. O., and Morimoto, R. I. (1996) *Science* **274**, 1718–1720
- Mücke, M., and Schmid, F. X. (1994) *J. Mol. Biol.* **239**, 713–725
- Kyte, J., and Doolittle, R. F. (1982) *J. Mol. Biol.* **157**, 105–132
- Gill, S. C., and von Hippel, P. H. (1989) *Anal. Biochem.* **182**, 319–326
- Atherton, E., Fox, H., Logan, C., J., Harkiss, D., Sheppard, R. C., and Williams, S. B. J. (1978) *Chem. Soc. Chem. Comm.* **13**, 537–539
- Knarr, G., Gething, M.-J., Modrow, S., and Buchner, J. (1995) *J. Biol. Chem.* **270**, 27589–27594
- Janowski, B., Wollner, S., Schutkowski, M., and Fischer, G. (1997) *Anal. Biochem.* **252**, 299–307
- Scholz, C., Rahfeld, J., Fischer, G., and Schmid, F. X. (1997) *J. Mol. Biol.* **273**, 752–762
- Scholz, C., Stoller, G., Zarnt, T., Fischer, G., and Schmid, F. X. (1997c) *EMBO J.* **16**, 54–58
- Buchner, J., Grallert, H., and Jakob, U. (1998) *Methods Enzymol.* **290**, 323–338
- Pierce, M. M., Raman, C. S., and Nall, B. T. (1999) *Methods* **19**, 213–221
- Yem, A. W., Reardon, I. M., Leone, J. W., Heinrikson, R. L., and Deibel, M. R. (1993) *Biochemistry* **32**, 12571–12576
- Chakrabarty, A., Kortemme, T., Padmanabhan, S., and Baldwin, R. L. (1993) *Biochemistry* **32**, 5560–5565
- Scholz, C., Schindler, T., Dolinsky, K., Heitman, J., and Schmid, F. X. (1997) *FEBS Lett.* **414**, 69–73
- Albers, M. W., Walsh, C. T., and Schreiber, S. L. (1990) *J. Org. Chem.* **55**, 4984–4986
- Horowitz, P. M. (1995) *Methods Mol. Biol.* **40**, 361–368
- O'Neil, K. T., and DeGrado, W. F. (1990) *Trends Biol. Sci.* **15**, 59–64
- Zarnt, T., Tradler, T., Stoller, G., Scholz, C., Schmid, F. X., and Fischer, G. (1997) *J. Mol. Biol.* **271**, 827–237
- Furutani, M., Ideno, A., Iida, T., and Maruyama, T. (2000) *Biochemistry* **39**, 453–462
- Goebel, M., and Yanagida, M. (1991) *Trends Biochem. Sci.* **16**, 173–177
- Brix, J., Ziegler, G. A., Dietmeier, K., Schneider-Mergener, J., Schulz, G. E., and Pfanner, N. (2000) *J. Mol. Biol.* **303**, 479–488
- Abe, Y., Shodai, T., Muto, T., Mihara, K., Torii, H., Nishikawa, S., Endo, T., and Kohda, D. (2000) *Cell* **100**, 551–560
- Santoro, M. M., and Bolen, D. W. (1988) *Biochemistry* **27**, 8063–8068